Baryogenesis in the two-Higgs doublet model

JHEP

Published by Institute of Physics Publishing for SISSA

Received: *June 1, 2006*
Revised: *August 10, 2006*
Accepted: *October 17, 2006*
Published: *November 14, 2006*

Baryogenesis in the two-Higgs doublet model

Lars Fromme,[a] **Stephan J. Huber**[b] **and Michael Seniuch**[a]

[a] *Fakultät für Physik, Universität Bielefeld*
D-33615 Bielefeld, Germany
[b] *Theory Division, CERN*
CH-1211 Geneva 23, Switzerland
E-mail: fromme@physik.uni-bielefeld.de, stephan.huber@cern.ch, seniuch@physik.uni-bielefeld.de

Abstract: We consider the generation of the baryon asymmetry in the two-Higgs doublet model. Investigating the thermal potential in the presence of CP violation, as relevant for baryogenesis, we find a strong first-order phase transition if the extra Higgs states are heavier than about 300 GeV. The mass of the lightest Higgs can be as large as about 200 GeV. We compute the bubble wall properties, including the profile of the relative complex phase between the two Higgs vevs. The baryon asymmetry is generated by top transport, which we treat in the WKB approximation. We find a baryon asymmetry consistent with observations. The neutron electric dipole moment is predicted to be larger than about 10^{-27} e cm and can reach the current experimental bound. Low values of $\tan\beta$ are favored.

Keywords: Baryogenesis, CP violation, Cosmology of Theories beyond the SM, Higgs Physics.

JHEP11(2006)038

Contents

1. Introduction

The origin of the baryon asymmetry of the universe (BAU) is still an open question in cosmology and particle physics. New measurements of the cosmic microwave background, combined with large-scale structure data, yield a baryon to entropy ratio of [1]

$$\eta_B \equiv \frac{n_B}{s} = (8.7 \pm 0.3) \times 10^{-11}. \tag{1.1}$$

Three necessary conditions, stated by Sakharov [2], have to be fulfilled for a dynamical generation of the baryon asymmetry: baryon number violation, C and CP violation, and departure from thermal equilibrium. In principle the standard model (SM) contains all these requirements, and the electroweak phase transition (EWPT) provides a natural mechanism for baryogenesis [3]. The baryon asymmetry is generated during the phase transition by electroweak sphaleron processes. To avoid subsequent baryon number washout, the sphaleron rate has to be suppressed after the phase transition. Hence the transition must be strongly first order, i.e. the expectation value of the Higgs field must be larger than about the critical temperature. In the SM there is no first-order phase transition for Higgs masses larger than about 80 GeV [4], far below the current experimental bound of 114 GeV [5]. The SM therefore fails to explain the baryon asymmetry. Moreover, the CP violation in the CKM matrix is too small to produce a sufficiently large baryon number [6].

Over the years there have been many proposals to realize electroweak baryogenesis in extended models (see, for instance, ref. [7] for a review). In supersymmetric theories, for example, a strong first-order PT can occur if the superpartner of the top quark is lighter than about 175 GeV [8], and the baryon asymmetry can be generated by chargino transport [9, 10]. Alternatively, the phase transition can be strengthened by the presence of SM singlets in the Higgs sector [11]. A more general effective field theory approach can

also be followed; there the Higgs sector is augmented by dimension-six operators to induce a first order phase transition and to provide additional CP violation [12 – 14].

In this paper we revisit electroweak baryogenesis in the two-Higgs doublet model (2HDM), paying special emphasis on the computation of the emerging baryon asymmetry. So far the most detailed study of this issue (for earlier work see ref. [15]) was performed in ref. [16]. Describing the interaction between the bubble wall and the plasma in terms of reflection and transmission coefficients, the authors concluded that the 2HDM is at best marginally capable of generating the observed baryon asymmetry. In contrast, we demonstrate that the WKB formalism, which is appropriate for thick walls, leads to a positive result. This is the main result of the present work.

In addition to the SM Higgs, the 2HDM contains two extra neutral and charged Higgs particles. If these extra states couple sufficiently strongly, their thermal loop corrections can induce a strong first-order phase transition [17 – 21]. In addition, a complex mass term, mixing the two Higgs doublets, provides a new source of CP violation, which fuels baryogenesis.

We examine the EWPT in the 2HDM, including explicit CP violation, using the finite temperature effective potential at one-loop order. In agreement with ref. [21], we find a strong phase transition for light Higgs masses of up to at least 200 GeV. The extra Higgses have to be heavier than about 300 GeV, depending somewhat on the model parameters. Turning on the CP-violating phase makes the phase transition slightly weaker. We determine the profile of the bubble wall, which separates the broken and symmetric phase. Except for the case of very strong phase transitions, we typically find thick bubble walls. The bubble wall is characterized by a varying complex phase between the two Higgs vevs. CP-violating interactions of the particles in the hot plasma, in particular the top quark, with the phase boundary then lead to different semiclassical forces acting on particles and antiparticles. Since we are dealing with thick bubble walls, we can apply the standard WKB formalism to compute the CP-violating source terms that enter the transport equations of electroweak baryogenesis [9, 22]. Here we use the formalism recently laid out in ref. [14], which makes sure that the correct dispersion relations of the Schwinger–Keldysh formalism [23] are reproduced. Also a finite W-scattering rate is included in the transport equations, which previously was set to equilibrium.

We find that a wide parameter range allows for the generation the observed baryon asymmetry. Since the model contains only a single CP-violating phase, we can predict the electric dipole moments of the neutron and electron. They are typically found to be below the current experimental bounds, but should be detectable in next-generation experiments.

2. The effective Higgs potential

In its most general form, the 2HDM suffers from flavor changing neutral currents at tree-level. To avoid this, a discrete symmetry, $\Phi_1 \to -\Phi_1$, $d_i^c \to \mp d_i^c$ (the other fields do not transform), is usually invoked [24], making sure that at most one Higgs doublet couples to the up- and down-type quarks, respectively. In the "$-$" case ("type II"), the down-type quarks couple only to Φ_1, while the up-type ones couple to Φ_2. In the other case ("type

I"), Φ_1 does not couple to the fermions at all. In the following only the coupling of the top quark will be relevant, so that we do not need to actually distinguish between types I and II. In section 4, where we will discuss electric dipole moments, we will focus on the type II case.

The most general potential is [25]

$$\begin{aligned} V_0(\Phi_1,\Phi_2) = & -\mu_1^2\Phi_1^\dagger\Phi_1 - \mu_2^2\Phi_2^\dagger\Phi_2 - \mu_3^2(e^{i\alpha}\Phi_1^\dagger\Phi_2 + \text{h.c.}) \\ & + \frac{\lambda_1}{2}(\Phi_1^\dagger\Phi_1)^2 + \frac{\lambda_2}{2}(\Phi_2^\dagger\Phi_2)^2 + \lambda_3(\Phi_1^\dagger\Phi_1)(\Phi_2^\dagger\Phi_2) \\ & + \lambda_4|\Phi_1^\dagger\Phi_2|^2 + \frac{\lambda_5}{2}\left((\Phi_1^\dagger\Phi_2)^2 + \text{h.c.}\right) \end{aligned} \tag{2.1}$$

and the Yukawa interactions read

$$\mathcal{L}_y = y\Phi_2 Q_3 t^c + \text{h.c.} + \ldots \tag{2.2}$$

Without loss of generality the couplings λ_i and the mass parameters μ_i can taken to be real. The mass term $\mu_3^2 e^{i\alpha}$ breaks the aforementioned Z_2 symmetry softly, without reintroducing tree-level flavor violation [26]. It can be complex, in which case the Higgs potential breaks CP. In total, the Higgs potential contains 9 parameters, which are 3 squared masses, 5 couplings, and 1 phase. One parameter is fixed by the Z-boson mass, leaving an 8-dimensional parameter space. The potential has to be bounded from below, which at tree-level translates into the constraints [20]

$$\lambda_1 > 0,\ \lambda_2 > 0,\ \sqrt{\lambda_1\lambda_2} + \lambda_3 > 0,\ \sqrt{\lambda_1\lambda_2} + \lambda_3 + \lambda_4 \pm \lambda_5 > 0. \tag{2.3}$$

Let us first consider the case $\alpha = 0$, i.e. the Higgs potential without CP violation. It has been shown that in this case no charge breaking minima exist, provided the charged Higgs mass squared is positive [27][1]. Later on we will assume that this result generalizes to the one-loop level, including a small CP-violating phase. We can therefore restrict ourselves to the neutral fields, which we parameterize as $\text{Re}\Phi_1^0 = h_1$ and $\text{Re}\Phi_2^0 = h_2$. The potential then reads

$$V_0(h_1,h_2) = -\mu_1^2 h_1^2 - \mu_2^2 h_2^2 - 2\mu_3^2 h_1 h_2 + \frac{\lambda_1}{2}h_1^4 + \frac{\lambda_2}{2}h_2^4 + (\lambda_3+\lambda_4+\lambda_5)h_1^2 h_2^2. \tag{2.4}$$

In the following we focus on the somewhat simpler case

$$\mu_1^2 = \mu_2^2,\ \lambda_1 = \lambda_2. \tag{2.5}$$

Moreover, this choice is favorable to generate large Higgs expectation values in the broken phase [17]. The Yukawa interaction (2.2) does not preserve these relations at the loop-level. At tree-level, eq. (2.5) implies the symmetry

$$\Phi_1 \leftrightarrow \Phi_2^\dagger, \tag{2.6}$$

[1] A study of symmetry breaking in a general 2HDM has recently been presented in ref. [28].

so that the minimum is at $\tan\beta \equiv \langle h_2\rangle/\langle h_1\rangle = 1$. With $\langle h_1\rangle = \langle h_2\rangle = h = 123$ GeV the extremal condition is then given by

$$-\mu_1^2 - \mu_3^2 + (\lambda_1+\lambda_3+\lambda_4+\lambda_5)h^2 = 0. \tag{2.7}$$

The mass matrix is block-diagonal and we obtain, besides 3 massless Goldstone bosons, 5 physical Higgs bosons. They consist of a pair of charged Higgses $H^\pm$, 2 neutral scalars h^0 and H^0, and a pseudoscalar A^0, with the corresponding squared masses as follows:

$$\begin{aligned} m_{H^\pm}^2 &= 2\mu_3^2 - 2(\lambda_4+\lambda_5)h^2, && (2.8)\\ m_{A^0}^2 &= 2\mu_3^2 - 4\lambda_5 h^2, && (2.9)\\ m_{H^0}^2 &= 2\mu_3^2 - 2(-\lambda_1+\lambda_3+\lambda_4+\lambda_5)h^2, && (2.10)\\ m_{h^0}^2 &= 2(\lambda_1+\lambda_3+\lambda_4+\lambda_5)h^2. && (2.11) \end{aligned}$$

These relations can be used to define the model in terms of μ_3^2 and the 4 Higgs masses.

In the case of non-vanishing α, CP is broken. We now parametrize the neutral Higgs fields as

$$\Phi_1^0 = h_1 e^{-i\theta_1},\ \Phi_2^0 = h_2 e^{i\theta_2}. \tag{2.12}$$

Note that the potential only depends on the combination $\theta = \theta_1 + \theta_2$. In the minimum we can always choose the gauge such that $\theta_1 = \theta_2 = \theta/2$. Still assuming the relations (2.5), the potential of the neutral fields reads

$$\begin{aligned} V_0(h_1,h_2,\theta) = &-\mu_1^2(h_1^2+h_2^2) - 2\mu_3^2 h_1 h_2\cos(\theta+\alpha) + \frac{\lambda_1}{2}(h_1^4+h_2^4)\\ &+(\lambda_3+\lambda_4+\lambda_5\cos(2\theta))h_1^2h_2^2. \end{aligned} \tag{2.13}$$

Using the notation $\langle\theta\rangle = \vartheta$, we obtain two extremal conditions,

$$\begin{aligned} -\mu_1^2 - \mu_3^2\cos(\vartheta+\alpha) + (\lambda_1+\lambda_3+\lambda_4+\lambda_5\cos(2\vartheta))h^2 &= 0\\ \mu_3^2\sin(\vartheta+\alpha) - \lambda_5\sin(2\vartheta)h^2 &= 0. \end{aligned} \tag{2.14}$$

The squared Higgs boson masses take the form

$$\begin{aligned} m_{H^\pm}^2 &= -2\mu_1^2 + 2(\lambda_1+\lambda_3)h^2,\\ m_{H_3}^2 &= -\mu_1^2 + 2(\lambda_1+\lambda_3+\lambda_4)h^2 + \sqrt{\mu_1^4 + 4\lambda_5\cos(2\vartheta)\mu_1^2h^2 + 4\lambda_5^2h^4},\\ m_{H_2}^2 &= -2\mu_1^2 + 4\lambda_1 h^2,\\ m_{H_1}^2 &= -\mu_1^2 + 2(\lambda_1+\lambda_3+\lambda_4)h^2 - \sqrt{\mu_1^4 + 4\lambda_5\cos(2\vartheta)\mu_1^2h^2 + 4\lambda_5^2h^4}. \end{aligned} \tag{2.15}$$

Note that the neutral Higgs states are now mixtures, with scalar and pseudoscalar contents. Again, these relations can be inverted to parameterize the model in terms of the Higgs masses, μ_3^2 and α.

At zero temperature the one-loop contribution to the effective potential is given by

$$V_1(\Phi_1,\Phi_2) = \sum_i \pm\frac{n_i}{64\pi^2} m_i^4 \ln\frac{m_i^2}{Q^2}, \tag{2.16}$$

where $m_i^2 = m_i^2(\Phi_1, \Phi_2)$ are field dependent mass eigenvalues, n_i is the corresponding number of degrees of freedom, and "+(−)" applies to bosonic (fermionic) contributions, respectively. We choose $Q = 246/\sqrt{2}$ GeV for the renormalization scale. We take only the heaviest bosons, i.e. $m_i = m_{H^\pm}, m_{H_2}, m_{H_3}$ ($n_{H^\pm} = n_{H_2} = n_{H_3} = 1$), and the fermion with the largest Yukawa coupling, i.e. $m_i = m_t$ ($n_t = 12$), into account. For the top quark mass we have $m_t^2 = y_t^2 \Phi_2^\dagger \Phi_2$. All other particles can be safely neglected, owing to their small contributions to the one-loop effective potential.

We add counter-terms to the potential, such that the tree-level minimum and Higgs masses are preserved at the one-loop level. This can be achieved by

$$\begin{aligned} V_{\rm CT}(\Phi_1, \Phi_2) = & -\delta\mu_1^2(\Phi_1^\dagger\Phi_1 + \Phi_2^\dagger\Phi_2) - \delta\mu_3^2(e^{i\alpha}\Phi_1^\dagger\Phi_2 + \text{h.c.}) \\ & + \frac{\delta\lambda_1}{2}(\Phi_1^\dagger\Phi_1)^2 + \frac{\delta\lambda_2}{2}(\Phi_2^\dagger\Phi_2)^2 + \delta\lambda_3(\Phi_1^\dagger\Phi_1)(\Phi_2^\dagger\Phi_2) \\ & + \delta\lambda_4|\Phi_1^\dagger\Phi_2|^2 + \frac{\delta\lambda_5}{2}\left((\Phi_1^\dagger\Phi_2)^2 + \text{h.c.}\right). \end{aligned} \tag{2.17}$$

In the following all Higgs masses are understood as being one-loop values. As already mentioned, the symmetry (2.6) no longer holds at the one-loop level, which we take care of by using $\delta\lambda_1 \neq \delta\lambda_2$. Three renormalization conditions are evidently given by

$$\left.\frac{\partial(V_1 + V_{\rm CT})}{\partial h_1}\right|_{\substack{h_1=h_2=h \\ \theta=\vartheta}} = \left.\frac{\partial(V_1 + V_{\rm CT})}{\partial h_2}\right|_{\substack{h_1=h_2=h \\ \theta=\vartheta}} = \left.\frac{\partial(V_1 + V_{\rm CT})}{\partial \theta}\right|_{\substack{h_1=h_2=h \\ \theta=\vartheta}} = 0, \tag{2.18}$$

meaning that the minimum of the potential $V = V_0 + V_1 + V_{\rm CT}$ does not change with respect to the tree-level case. Preserving the values of the Higgs masses, which we compute from the second derivatives of V, provides another four conditions. So the coefficients of $V_{\rm CT}$ are fixed. Since the conditions related to Higgs masses include non-linearities, the resulting equations for the counter-terms have to be solved numerically.

The 2HDM is subject to a number of experimental constraints. In the considered parameter range, the lightest Higgs boson is SM-like, and therefore its mass has to obey the lower LEP bound of 114 GeV [5]. The 2HDM does not respect the custodial symmetry of the SM. So there is the danger of large corrections to the electroweak precision observables. These corrections can be approximately described in terms of contributions to the self-energies, the so called "oblique" corrections. The relevant expressions for the 2HDM with CP-violation can be found in ref. [29]. To be consistent with observations, the mass splittings between the extra Higgs states should not be much larger than the W-mass. Later on we will set these masses equal to reduce the number of parameters. Oblique corrections then are automatically small. Another important constraint comes from $b \to s\gamma$, which in the type II model requires $m_{H^\pm} \gtrsim 200$ GeV [30][2]. Constraints from the muon anomalous magnetic moment [32] and from tau decays [33] are not relevant for the low values of $\tan\beta$, which we consider.

At finite temperature the one-loop contribution to the effective potential is given by

$$V_1^T = T^4 \sum_B n_B \, f_B\left(\frac{m_B}{T}\right) + T^4 \sum_F n_F \, f_F\left(\frac{m_F}{T}\right), \tag{2.19}$$

[2]One can also consider constraints from $B_d^0 - \bar{B}_d^0$ mixing [31].

where $n_{B(F)}$ counts the positive degrees of freedom for bosons (fermions). In the high temperature limit, $m/T \ll 1$, one obtains [34]

$$f_B^{\rm HT}\left(\frac{m}{T}\right) \approx \frac{-\pi^2}{90} + \frac{m^2}{24T^2} - \frac{m^3}{12\pi T^3} - \frac{m^4}{64\pi^2 T^4}\ln\left(\frac{m^2}{c_B T^2}\right) \tag{2.20}$$

$$f_F^{\rm HT}\left(\frac{m}{T}\right) \approx \frac{-7\pi^2}{720} + \frac{m^2}{48T^2} + \frac{m^4}{64\pi^2 T^4}\ln\left(\frac{m^2}{c_F T^2}\right), \tag{2.21}$$

with $c_F = \pi^2 \exp(3/2 - 2\gamma_e) \approx 13.94$ and $c_B = 16 c_F$, and in the low temperature limit, when m/T is large,

$$f^{\rm LT}\left(\frac{m}{T}\right) \approx -\left(\frac{m}{2\pi T}\right)^{3/2} \exp\left(-\frac{m}{T}\right)\left(1 + \frac{15m}{8T}\right). \tag{2.22}$$

In this low temperature limit the contributions from bosons and fermions have the same asymptotic behavior.

We use these approximations because they are much more convenient to handle than the full integral expressions of ref. [34]. It turns out, however, that these limiting cases are not sufficient since some states cross from the high temperature to the low temperature regime. For an expression to be valid in the whole temperature range, we therefore use a smooth interpolation between the low- and high-T limits. For bosons we use eq. (2.20) for $m/T < 1.8$ and eq. (2.22) for $m/T > 4.5$, and for fermions eq. (2.21) for $m/T < 1.1$ and eq. (2.22) for $m/T > 3.4$. The interpolations are made in such a way that the functions as well as their derivatives match at the connecting points. The deviation between our approximation and the exact solution is less than 4%. Finally, the effective potential is given by

$$V_{\rm eff} = V_0 + V_1 + V_{\rm CT} + V_1^T. \tag{2.23}$$

In V_1^T we also take into account the contributions of W-bosons ($n_W = 6$) and Z-bosons ($n_Z = 3$). In perturbation theory the strength of a strong phase transition would be underestimated by resummation of the gauge boson contributions [35]. Therefore we do not resum these corrections to compensate for non-perturbative effects. In ref. [21] the thermal contributions of the heavy Higgs bosons have been resummed, using the high temperature approximation for the thermal Higgs masses. We find that in the broken minimum the high temperature approximation is often not justified for the heavy Higgs states. Ignoring this fact, and nevertheless resumming the Higgs contributions by using thermal masses instead of the bare masses in eq. (2.19), we find a phase transition less than 15% weaker than in unresummed case. The effect is marginal for large heavy Higgs masses and becomes stronger for smaller ones. Including the light Higgs and the Goldstone bosons has an even smaller effect. In the results we present below, the Higgs contributions are not resummed.

3. The phase transition

The dynamics of the EWPT is governed by $V_{\rm eff}(h_1, h_2, \theta, T)$. The critical temperature, T_c, of a first-order phase transition is defined by the condition that the effective potential has

two degenerate minima, the symmetric minimum at $\langle h_1\rangle_T = \langle h_2\rangle_T = 0$ and the broken minimum at $\langle h_1\rangle_T = v_1 > 0$ and $\langle h_2\rangle_T = v_2 > 0$, which are separated by an energy barrier. The total Higgs expectation value we define by $v_c = \sqrt{2}\sqrt{v_1^2 + v_2^2}$, where the factor $\sqrt{2}$ is due to our normalization of the Higgs fields. Somewhat below T_c, at the nucleation temperature T_n, bubbles of the broken phase start to nucleate and expand. Baryogenesis takes place outside the bubbles in the symmetric phase while, inside the bubbles, the sphaleron rate that provides $(B+L)$-violating processes has to be switched off. Otherwise the baryon asymmetry will be washed out after the phase transition. In order to preserve the created baryon asymmetry, the washout criterion [36]

$$\xi = \frac{v_c}{T_c} \gtrsim 1 \tag{3.1}$$

must hold, i.e. the phase transition has to be sufficiently strong.

In the following we analyze the parameter space with respect to the strength ξ of the phase transition. We focus on the case of degenerate heavy Higgs masses, which reduces the dimension of the parameter space. As noted in the previous section, this choice has the additional benefit to keep oblique corrections automatically small. At tree-level this means that $\lambda_1(=\lambda_2) = \lambda_3$ and $\lambda_4 = \lambda_5$. As input parameters we take $\mu_3^2, \alpha, m_h = m_{H_1}$, and $m_H = m_{H_2} = m_{H_3} = m_{H^\pm}$. One finds that for larger values of α ($\alpha = 0.4$ for example) the first-order phase transition can change into a two-stage transition if the heavy Higgs mass is sufficiently small. The potential then shows an additional local minimum. The phase transition proceeds by a second-order phase transition from the symmetric phase to this extra minimum, followed by a first-order phase transition to the low temperature broken phase[3]. We exclude these values from the parameter space and only define the strength ξ in the case of a pure first-order PT.

Another important property that enters the transport equations discussed in section 5 is the wall profile of the expanding bubbles. If the nucleating bubbles have reached a sizable extent and expand with constant velocity, we can boost into the rest frame of the bubble wall and assume a planar wall. In principle one has to numerically solve the field equations of the Higgs fields, using an algorithm such as the one recently proposed in ref. [37]. To achieve a sufficiently strong phase transition we are led to $m_H^2 \gg m_h^2$. The effective potential is then characterized by a valley, corresponding to the single light Higgs field. During the phase transition the fields will follow this valley very closely, in order not to feel the heavy Higgs masses. So we can approximate the phase transition by single field dynamics. Numerically we determine the valley by minimizing the thermal potential at T_c with respect to h_2 and θ at fixed values of h_1 between the symmetric and broken phase. For a simple φ^4 model, with one real scalar field φ and a broken minimum at v_c, the wall profile is exactly described by a kink solution,

$$\varphi(z) = \frac{v_c}{2}\left(1 - \tanh\frac{z}{L_\mathrm{w}}\right), \tag{3.2}$$

[3]The second-transition is in general too weak to avoid baryon number washout. Also, the non-zero Higgs vev outside the bubbles would lead to a suppression of the sphaleron rate and therefore also of the baryon asymmetry. So the two-stage transition does not allow us to generate the baryon asymmetry.

with a wall thickness $L_{\rm w} = \sqrt{v_c^2/(8V_b)}$, where V_b is the height of the potential barrier and z is the coordinate orthogonal to the wall. We use this approximation for $L_{\rm w}$, determining V_b as the maximal height of the potential barrier along the valley connecting the two minima.

Let us now briefly discuss the behavior of $L_{\rm w}$ and ξ with the input parameters. We require $m_h \geq 115$ GeV to be consistent with the LEP bound on the Higgs mass. For increasing m_H and keeping the other parameters fixed, the wall thickness decreases, while the PT becomes stronger. This somewhat counter-intuitive result is due to the fact that the larger Higgs masses (2.15) come from larger quartic couplings. So this limit actually does not lead to the decoupling of the heavy states. At some point perturbation theory will finally break down. Later on, when computing the baryon asymmetry, we will face another constraint. The gradient expansions is justified only for thick bubble walls, so we will require $L_{\rm w}T_c > 2$. In practice this leads to an upper bound on m_H similar to the perturbativity constraint.

In figures 1–3 constant lines of ξ and $L_{\rm w}$ are shown in the dependence of m_h and m_H for different values of μ_3^2 and α. The influence of the CP-violating phase α on ξ and $L_{\rm w}$ is rather small, as can be seen from figures 1 and 2. For small values of ξ, or large values of $L_{\rm w}$, the lines are marginally shifted upwards. This behavior continues for increasing α. If we choose $\alpha = 0.4$ the effect is negligible above $\xi \approx 1.5$, but below $\xi \approx 1.3$ the PT changes into a two-stage one. The effect of increasing μ_3^2 is a shift to higher values for m_H. The comparison of $\mu_3^2 = 10000$ GeV^2 and 20000 GeV^2, e.g. figures 2 and 3, shows that the range of m_H is moved to higher values, while the extent shrinks by around 20 GeV. Using a larger value of μ_3^2 means that the same quartic couplings lead to heavier Higgses. The strength of the phase transition is more governed by the size of the quartic couplings than by the actual value of m_H. Notice that here the bound on the charged Higgs mass from $b \to s\gamma$, which we discussed above, is automatically satisfied in the case of a strong phase transition.

As stated in the previous section, in this analysis we neglect the lightest Higgs boson due to its small contribution to the effective potential. This a conservative prescription, as including the lightest Higgs state, the phase transition turns out be slightly stronger. The influence of the lightest Higgs depends on the strength of the phase transition and is almost independent of m_h. For $\xi \sim 1$, including the lightest Higgs state enhances the strength of the phase transition, i.e. ξ by about 9%. For a stronger phase transition of $\xi \sim 2$ the increase drops to about 3%. This behavior is expected, as in the latter case the dynamics is much more dominated by the heavy Higgs states. In any case the effect of the lightest Higgs state is within the errors of the one-loop approximation.

In figures 1 and 2 the one-loop corrections $\Delta = \max|\delta\lambda_i/\lambda_i|$ to the quartic couplings, i.e. the size of the counter-terms with respect to the tree-level terms, range from 15% for $m_H = 300$ GeV to 50% for $m_H = 440$ GeV. This means that in the case of a very strong phase transition, perturbation theory starts to break down and sizable corrections to our results have to be expected. For $\xi \sim 1$ higher-order corrections are well under control. These results agree with the findings of ref. [21]. In conclusion, we find that a wide range of parameters fulfills the requirements of electroweak baryogenesis.

Up to now we have only discussed observables involving the fields h_1 and h_2. However,

JHEP11(2006)038

also the CP-violating phase θ, which varies along the bubble wall from $\theta_{\rm sym}$ to $\theta_{\rm brk}$, is essential for baryogenesis. According to the above discussion, we compute the θ-profile approximately by minimizing the thermal potential at T_c with respect to h_2 and θ at fixed values of h_1 between the symmetric and broken phase. As a representative example we show in figure 4a the θ-profile parametrized by h_1 for the set $\mu_3^2 = 10000\ \mathrm{GeV}^2$ and $\alpha = 0.2$. There, θ changes from $\theta_{\rm sym} = -0.29$ to $\theta_{\rm brk} = -0.06$, which is indicated by the dotted lines. In a simplified manner, we describe the θ-profile by a kink ansatz, i.e.

$$\theta(z) = \theta_{\rm brk} - \frac{\Delta\theta}{2}\left(1 + \tanh\frac{z}{L_{\rm w}}\right), \tag{3.3}$$

using the derived wall thickness $L_{\rm w}$ and $\Delta\theta = \theta_{\rm brk} - \theta_{\rm sym}$. The CP violation in the Higgs sector gives rise to complex fermion masses, which change while the particles pass through the bubble wall. We only take into account the top quark as the heaviest fermion. With our parametrization (2.12) of the neutral Higgs components, one finds for the complex top mass

$$\mathcal{M}_t(z) = y_t h_2(z)\, e^{i\theta(z)/2} = y_t \frac{h(z)}{\sqrt{2}} \sin\beta_T\, e^{i\theta(z)/2} = m_t(z)\, e^{i\theta_t(z)}, \tag{3.4}$$

where β_T is the angle between h_1 and h_2 at T_c, i.e. $\tan\beta_T = v_2/v_1$, which is less, but rather close to 1. The top Yukawa coupling y_t is chosen such that the top mass at zero temperature is 173 GeV. In general, the change in $\theta_2 (= \theta_t)$ along the bubble wall is given by $\Delta\theta_2 = \Delta\theta/(1 + \tan^2\beta_T)$, assuming that $\tan\beta_T$ is constant along the wall [38]. So there is an additional suppression for $\Delta\theta_2$ for large $\tan\beta$. $\mathcal{M}_t$ enters the computation of the baryon asymmetry; in particular, the derivative of $\theta_t(z)$ induces the CP-violating the source term. Therefore a large value of $\Delta\theta$ enhances the baryon asymmetry. As shown in figure 4b, $\Delta\theta$ strongly depends on m_h. Raising m_h or m_H does increase the change in θ. We also find that $\Delta\theta$ depends almost linearly on the coupling α, whereas the influence of μ_3^2 is small. Notice that $\Delta\theta$ can be larger than the input phase α.

4. Electric dipole moments

CP violation induces electric dipole moments (EDMs). The latest experimental limits for the neutron [39] and electron [40] EDMs at 90% confidence level are

$$|d_n| \leq 3.0 \times 10^{-26}\ e\,\mathrm{cm}, \tag{4.1}$$

$$|d_e| \leq 1.6 \times 10^{-27}\ e\,\mathrm{cm}. \tag{4.2}$$

In the standard model the only source of CP violation originates from the Kobayashi-Maskawa matrix in the quark sector. Contributions to the EDMs arise first at the three-loop level, which results in a natural suppression, several orders of magnitude below current bounds. EDMs are therefore an ideal probe of new physics.

In the 2HDM, EDMs are induced by scalar–pseudoscalar mixing in the neutral Higgs sector. The contributions to the EDMs can be computed in terms of parameters $\mathrm{Im}(Z)$, which measure the degree of CP non-conservation and which are the imaginary parts of

Higgs fields normalization constants [41]. The four CP-violating parameters

$$\mathrm{Im}(Z_{0i}), \quad \mathrm{Im}(\widetilde{Z}_{0i}), \quad \mathrm{Im}(Z_{1i}), \quad \mathrm{Im}(Z_{2i}), \tag{4.3}$$

where i indicates each of the four neutral Higgs bosons, enter the calculation of the EDMs. They can be expressed in terms of components of the neutral Higgs mass matrix eigenvectors. The Goldstone boson does not contribute to these factors, since the corresponding Z's are real. Thus, the sum can be restricted to the three massive neutral bosons. Note that the parameters respect in addition the sum rules [41]

$$\sum_i \mathrm{Im}(Z_{0i}) = \sum_i \mathrm{Im}(\widetilde{Z}_{0i}) = \sum_i \mathrm{Im}(Z_{1i}) = \sum_i \mathrm{Im}(Z_{2i}) = 0, \tag{4.4}$$

which means that CP violation vanishes if the masses of the neutral Higgs bosons are degenerate.

In the 2HDM the dominant contributions to the electron EDM are two-loop amplitudes, which were first computed by Barr and Zee [42]. They demonstrated that the effect is enhanced with respect to the standard one-loop contributions [43]. Further two-loop diagrams, including the W-boson, were taken into account in investigations by Gunion and Vega [44], Chang et al. [45], as well as Leigh et al. [46]. In this work we use the results of Chang et al., ignoring some minor corrections discussed in ref. [46]. We end up with the following contributions

$$\begin{aligned} d_e/e = {} & (d_e/e)^{H\gamma\gamma}_{t-\mathrm{loop}} + (d_e/e)^{HZ\gamma}_{t-\mathrm{loop}} + (d_e/e)^{H\gamma\gamma}_{W-\mathrm{loop}} \\ & + (d_e/e)^{HZ\gamma}_{W-\mathrm{loop}} + (d_e/e)^{H\gamma\gamma}_{G-\mathrm{loop}} + (d_e/e)^{HZ\gamma}_{G-\mathrm{loop}}. \end{aligned} \tag{4.5}$$

When computing the EDM of the neutron one has to deal with hadronic effects, which make its relation to the partonic EDMs difficult. Various proposals have been made in the literature how to perform this calculation (see ref. [47] for a recent review). The dominant contributions to the neutron EDM come from the color EDMs (CEDMs) of the constituent quarks $\tilde{d}_k$, $k = u, d$ [48],

$$\mathcal{L} \supset -\frac{i}{2}\tilde{d}_k g_s \bar{\psi}_k \sigma_{\mu\nu} G^{\mu\nu} \gamma_5 \psi_k = \frac{1}{2}\tilde{d}_k g_s \bar{\psi}_k \sigma_{\mu\nu} \tilde{G}^{\mu\nu} \psi_k, \tag{4.6}$$

and from Weinberg's three-gluon operator [41]

$$\mathcal{L} \supset \frac{1}{3} w f^{abc} G^a_{\mu\nu} \tilde{G}^{\nu\beta,b} G^{\mu,c}_{\beta}. \tag{4.7}$$

The QCD-corrected coefficients $\tilde{d}_u$, $\tilde{d}_d$ and w are given by 2-loop calculations [48 – 51]. Using the results of [47], based on QCD sum rule techniques, the neutron EDM reads

$$(d_n/e)(\tilde{d}_u, \tilde{d}_d) = (1 \pm 0.5)(0.55\tilde{d}_u + 1.1\tilde{d}_d) \tag{4.8}$$

and

$$|(d_n/e)(w)| = 22 \text{ MeV } |w|. \tag{4.9}$$

Thus there is an error of about 50% in $(d_n/e)(\tilde{d}_u, \tilde{d}_d)$ and furthermore an error of about 100% in $(d_n/e)(w)$. Moreover, it is not possible to determine the sign of $(d_n/e)(w)$. Fortunately, this latter contribution turns out to be small (typically a 1% correction). The same is true for the contributions of the quark EDMs d_u and d_d (typically a 10% correction).

Let us now discuss the relevance of the electron and neutron EDMs for the 2HDM. One finds that in the analyzed parameter region the value of d_e is about five to thirty times smaller than the experimental limit of 1.6×10^{-27} $e\,\mathrm{cm}$. Thus, there emerges no additional constraint on the parameters. Let us focus on the importance of the different contributions to d_e and on the dependence of d_e on the input parameters. Since an EDM arises because of CP violation, we expect a larger value for an increasing CP phase α. Indeed we find that d_e approximately doubles if we change α from 0.2 to 0.4. Also raising μ_3^2 enhances d_e. Concerning the single contributions to d_e the largest ones originate from the top- and W-loops, with $(d_e)_{W-\mathrm{loop}} > 0$ whereas $(d_e)_{t-\mathrm{loop}} < 0$. The absolute value of $(d_e)_{t-\mathrm{loop}}$ is somewhat smaller, but of similar magnitude as $(d_e)_{W-\mathrm{loop}}$. So the sum is a factor of about 5–10 smaller than each individual contribution, and is then of the same order of magnitude as the Goldstone-loop contribution. Thus, all three parts are important for the electron EDM. We observe this behavior in the whole analyzed parameter region. We also investigate the dependence of d_e on the Higgs masses. For increasing both, m_h and m_H, the value of d_e decreases. This tendency becomes apparent in figure 5 where we compare lines of constant electron and neutron EDMs in the m_h–m_H plane. We find that the larger μ_3^2, the weaker is the dependence on the heavy Higgs mass.

Similar to the electron EDM, the one of the neutron also lies below its experimental bound of 3.0×10^{-26} $e\,\mathrm{cm}$ in the analyzed parameter region. But in contrast to d_e it almost reaches this experimental limit. However, note that d_n has quite a large error of about 50%, as pointed out. The limit of 3.0×10^{-26} $e\,\mathrm{cm}$ is just saturated in the case of $\mu_3^2 = 20000\ \mathrm{GeV}^2$ and $\alpha = 0.4$, for small Higgs masses. However, since the error band is large, there actually arises no constraint. For larger values of μ_3^2 or α, the neutron EDM of course increases and may exceed the measured bound in a wider mass range. The dependence of the neutron EDM on the input parameters is quite similar to that of the electron EDM. The lines of constant d_n run approximately parallel to those of d_e in the m_h–m_H plane; the slope is just a little flatter. We also find roughly a doubling for a change in α from 0.2 to 0.4. The dominant contribution arises from the color EDM of the down-quark, which is about a factor 3.5 larger than the one due to the up-quark CEDM. The part $|d_n(w)|$ arising from the three-gluon operator is roughly an order 1% correction and can therefore be neglected. In summary, for the considered parameter ranges, both the electron and neutron electric dipole moments lie below the experimental limits. The value of d_e is about one order of magnitude below the observational bound, and because of the large error in the theoretical determination of d_n, it also does not definitely exceed the bound set by experiments.

JHEP11(2006)038

5. Transport equations

In this section we discuss the evolution of the particle distributions during the phase transition. The CP-violating interactions of particles in the plasma with the bubble wall create an excess of left-handed quarks over the corresponding antiquarks. This excess diffuses into the symmetric phase, where the left-handed quark density biases the sphaleron transitions to generate a net baryon asymmetry.

Using the semiclassical WKB formalism [9, 14, 22], we obtain different dispersion relations for particles and antiparticles in the space-time dependent background of the Higgs expectation values. The dispersion relations then lead to force terms in the transport equations. The WKB method is justified when the de Broglie wavelength of the particles in the plasma is much shorter than the bubble wall thickness [22]. Hence the condition $L_{\rm w}T \gg 1$ has to be satisfied to legitimate an expansion in derivatives of the background Higgs fields. As demonstrated in section 3 we find that a large part of the parameter space does fulfill this condition.

In the 2HDM, baryogenesis is driven by top transport. So we can focus the discussion on the case of a single Dirac fermion, with a space-time dependent mass $\mathrm{Re}\mathcal{M}(z) + i\gamma^5\mathrm{Im}\mathcal{M}(z)$, where $\mathcal{M}(z) = m(z)e^{i\theta(z)}$. The dispersion relation to first order in gradients is given by [14, 23]

$$E = E_0 \pm \Delta E = E_0 \mp s\frac{\theta' m^2}{2E_0 E_{0z}}, \tag{5.1}$$

where $E_0 = \sqrt{\mathbf{p}^2 + m^2}$ and $E_{0z} = \sqrt{p_z^2 + m^2}$ in terms of the kinetic momentum. The prime denotes the derivative with respect to z, and the upper and the lower sign corresponds to particles and antiparticles, respectively. The spin factor $s = 1$ (-1) for z-spin up (down) is related to the helicity λ by $s = \lambda\,\mathrm{sign}(p_z)$. Note that eq. (5.1) is the dispersion relation in a general Lorentz frame, in contrast to the one derived in ref. [9]. For the group velocity of the WKB wave-packet one obtains

$$v_{gz} = \frac{p_z}{E_0}\left(1 \pm s\frac{\theta'}{2}\frac{m^2}{E_0^2 E_{0z}}\right). \tag{5.2}$$

The semiclassical force acting on the particles,

$$F_z = -\frac{(m^2)'}{2E_0} \pm s\frac{(m^2\theta')'}{2E_0 E_{0z}} \mp s\frac{\theta' m^2 (m^2)'}{4E_0^3 E_{0z}}, \tag{5.3}$$

results from the canonical equations of motion. It was the main result of ref. [14] that the expressions for the dispersion relation (5.1), the group velocity (5.2), and the semiclassical force (5.3) agree with the full Schwinger–Keldysh result [23].

In the semiclassical approximation the evolution of the particle distributions f_i is described by a set of classical Boltzmann equations. We assume a planar wall moving with constant velocity $v_{\rm w}$. Hence, in the rest frame of the wall, the distributions f_i only depend on z, p_z and $p = |\mathbf{p}|$, due to the translational invariance parallel to the wall. For each fluid of particle type i we have

$$(v_{gz}\partial_z + F_z\partial_{p_z})f_i = \mathbf{C}_i[f], \tag{5.4}$$

without any explicit time dependence, as we are looking for a stationary solution. The $\mathbf{C}_i$ are the collision terms describing the change of the phase-space density by particle interactions that drive the system back to equilibrium. We introduce perturbations around the chemical and kinetic equilibrium with the fluid-type truncation in the rest frame of the wall [9]

$$f_i(z, p_z, p) = \frac{1}{e^{\beta[\gamma_w(E_i + v_\mathrm{w} p_z) - \mu_i]} \pm 1} + \delta f_i(z, p_z, p) \tag{5.5}$$

where $\beta = 1/T$ and $\gamma_\mathrm{w} = 1/\sqrt{1 - v_\mathrm{w}^2}$, and plus (minus) refers to fermions (bosons). Here the chemical potentials $\mu_i(z)$ model a local departure from the equilibrium particle density and the perturbations δf_i describe the movement of the particles in response to the force. The latter do not contribute to the particle density, i.e. $\int d^3p\ \delta f_i = 0$. To first order in derivatives the perturbations are CP-even and equal for particles and antiparticles. But to second order they have CP-even and CP-odd parts, which we treat separately, i.e.

$$\mu_i = \mu_{i,1e} + \mu_{i,2o} + \mu_{i,2e}, \qquad \delta f_i = \delta f_{i,1e} + \delta f_{i,2o} + \delta f_{i,2e}, \tag{5.6}$$

so that the perturbations to second order for particles differ from those for antiparticles.

In order to compute the asymmetry in the left-handed quark density, we expand the Boltzmann equation in gradients. In the model under consideration, the most important particle species are top and bottom quarks, as well as the Higgs bosons. The other quark flavors and the leptons can be neglected thanks to their small Yukawa couplings. In a first step we assume baryon number conservation. We take into account W-scatterings, the top Yukawa interaction, the strong sphalerons, the top helicity flips and Higgs number violation with rates Γ_W, Γ_y, Γ_{ss}, Γ_m and Γ_h, respectively, where the latter two are only present in the broken phase. After the left-handed quark asymmetry is computed, the weak sphalerons, with the rate Γ_{ws}, convert it into a baryon asymmetry.

We follow the computation and notation presented in ref. [14]. We weight the Boltzmann equations with 1 and p_z/E_0, and perform the momentum average. Accordingly "plasma velocities" appear in the following, which are defined as $u_i \equiv \langle (p_z/E_0)\delta f_i \rangle$. We end up with the transport equations for chemical potentials of left-handed SU(2) doublet tops $\mu_{t,2}$, left-handed SU(2) doublet bottoms $\mu_{b,2}$, left-handed SU(2) singlet tops $\mu_{t^c,2}$, Higgs bosons $\mu_{h,2}$, and the corresponding plasma velocities

$$\begin{aligned}
&3v_\mathrm{w} K_{1,t}\mu'_{t,2} + 3v_\mathrm{w} K_{2,t}(m_t^2)'\mu_{t,2} + 3u'_{t,2} \\
&-3\Gamma_y(\mu_{t,2} + \mu_{t^c,2} + \mu_{h,2}) - 6\Gamma_m(\mu_{t,2} + \mu_{t^c,2}) - 3\Gamma_W(\mu_{t,2} - \mu_{b,2}) \\
&-3\Gamma_{ss}[(1 + 9K_{1,t})\mu_{t,2} + (1 + 9K_{1,b})\mu_{b,2} + (1 - 9K_{1,t})\mu_{t^c,2}] = 0
\end{aligned}$$

$$\begin{aligned}
&3v_\mathrm{w} K_{1,b}\mu'_{b,2} + 3u'_{b,2} \\
&-3\Gamma_y(\mu_{b,2} + \mu_{t^c,2} + \mu_{h,2}) - 3\Gamma_W(\mu_{b,2} - \mu_{t,2}) \\
&-3\Gamma_{ss}[(1 + 9K_{1,t})\mu_{t,2} + (1 + 9K_{1,b})\mu_{b,2} + (1 - 9K_{1,t})\mu_{t^c,2}] = 0
\end{aligned}$$

$$\begin{aligned}
&3v_\mathrm{w} K_{1,t}\mu'_{t^c,2} + 3v_\mathrm{w} K_{2,t}(m_t^2)'\mu_{t^c,2} + 3u'_{t^c,2} \\
&-3\Gamma_y(\mu_{t,2} + \mu_{b,2} + 2\mu_{t^c,2} + 2\mu_{h,2}) - 6\Gamma_m(\mu_{t,2} + \mu_{t^c,2})
\end{aligned}$$

$$
\begin{aligned}
-3\Gamma_{ss}[(1+9K_{1,t})\mu_{t,2}+(1+9K_{1,b})\mu_{b,2}+(1-9K_{1,t})\mu_{t^c,2}] &= 0 \\
4v_{\rm w}K_{1,h}\mu'_{h,2}+4u'_{h,2} & \\
-3\Gamma_y(\mu_{t,2}+\mu_{b,2}+2\mu_{t^c,2}+2\mu_{h,2})-4\Gamma_h\mu_{h,2} &= 0 \qquad (5.7) \\
-3K_{4,t}\mu'_{t,2}+3v_{\rm w}\tilde{K}_{5,t}u'_{t,2}+3v_{\rm w}\tilde{K}_{6,t}(m_t^2)'u_{t,2}+3\Gamma_t^{\rm tot}u_{t,2} &= S_t \\
-3K_{4,b}\mu'_{b,2}+3v_{\rm w}\tilde{K}_{5,b}u'_{b,2}+3\Gamma_b^{\rm tot}u_{b,2} &= 0 \\
-3K_{4,t}\mu'_{t^c,2}+3v_{\rm w}\tilde{K}_{5,t}u'_{t^c,2}+3v_{\rm w}\tilde{K}_{6,t}(m_t^2)'u_{t^c,2}+3\Gamma_t^{\rm tot}u_{t^c,2} &= S_t \\
-4K_{4,h}\mu'_{h,2}+4v_{\rm w}\tilde{K}_{5,h}u'_{h,2}+4\Gamma_h^{\rm tot}u_{h,2} &= 0. \qquad (5.8)
\end{aligned}
$$

Here the second-order perturbations label the difference between particles and antiparticles, i.e. $\mu_2 = \mu_{2o} - \bar{\mu}_{2o}$ and $u_2 = u_{2o} - \bar{u}_{2o}$. On the r.h.s., S_t denotes the source term of the top quark,

$$
S_t = -v_{\rm w}K_8(m_t^2\theta'_t)' + v_{\rm w}K_9\theta'_t m_t^2(m_t^2)'. \qquad (5.9)
$$

The source term of the bottom quark, which is suppressed by $m_b^2/m_t^2 \sim 10^{-3}$, has been neglected. The Higgs bosons do not have a source term to second order in gradients. The various thermal averages K_i in eqs. (5.7), (5.8) and (5.9) are defined similarly to ref. [14]. We include the position dependence of the K_i. The damping of $u_{i,2}$ can be approximated by the total interaction rate, $\Gamma_i^{\rm tot}$. In the numerical evaluations we have included a term $3\Gamma_W(u_{t,2}-u_{b,2})$ which affects results only at the few percent level. Contrary to the transport equations in ref. [14] we have doubled the degrees of freedom of the Higgs bosons to account for the second Higgs doublet in the model.

Using baryon number conservation, the chemical potential of left-handed quarks can be expressed in terms of the solutions of the transport equations $\mu_{t,2}$, $\mu_{b,2}$ and $\mu_{t^c,2}$,

$$
\begin{aligned}
\mu_{B_L} &= \mu_{q_1,2}+\mu_{q_2,2}+\frac{1}{2}(\mu_{t,2}+\mu_{b,2}) \\
&= \frac{1}{2}(1+4K_{1,t})\mu_{t,2}+\frac{1}{2}(1+4K_{1,b})\mu_{b,2}-2K_{1,t}\mu_{t^c,2}. \qquad (5.10)
\end{aligned}
$$

Now, in a second step, the weak sphalerons convert the left-handed quark number into a baryon asymmetry.

6. The baryon asymmetry

The baryon asymmetry is obtained by [9]

$$
\eta_B = \frac{n_B}{s} = \frac{405\Gamma_{ws}}{4\pi^2 v_{\rm w} g_* T}\int_0^\infty dz\ \mu_{B_L}(z)e^{-\nu z}. \qquad (6.1)
$$

Γ_{ws} is the weak sphaleron rate, which is only present in the symmetric phase, and $g_* = 106.75$ is the effective number of degrees of freedom in the plasma. The exponent $\nu =$

$45\Gamma_{ws}/(4v_{\rm w})$ accounts for the relaxation of the baryon number in case of a slowly moving wall.

In our evaluation we use the values $\Gamma_{ws} = 1.0 \times 10^{-6}$ for the weak sphaleron rate [52], $\Gamma_{ss} = 4.9 \times 10^{-4} T$ for the strong sphaleron rate [53], $\Gamma_y = 4.2 \times 10^{-3} T$ for the top Yukawa rate [54], $\Gamma_m = m_t^2(z,T)/(63T)$ for the top helicity flip rate [54], and $\Gamma_h = m_W^2(z,T)/(50T)$ for the Higgs number violation rate [54]. Furthermore the total interaction rate can be expressed by the diffusion constant, $\Gamma_i^{\rm tot} = (D_i K_{1,i})/K_{4,i}$, where the quark diffusion constant is given by $D_q = 6/T$ [54] and the Higgs diffusion constant by $D_h = 20/T$ [9]. The finite W-scattering rate we approximate as $\Gamma_W = \Gamma_h^{\rm tot}$. The bottom quark and the Higgs bosons are taken as massless.

Figure 6 displays the baryon asymmetry as a function of the wall velocity $v_{\rm w}$ for one typical parameter set. The solid line indicates the solution when using the full set of transport equations (5.7) and (5.8). If we resubstitute $E_{0z} \to E_0$ in the dispersion relation (5.1), the group velocity (5.2) and the semiclassical force (5.3), i.e. going back to these quantities as determined in ref. [9], the resulting baryon asymmetry is substantially reduced (dashed line). This confirms the recent result that performing the boost back to a general Lorentz frame has a sizable effect and should not be neglected [14]. In addition we have improved the transport equations by keeping a finite W-scattering rate. If these interactions were in equilibrium, η_B would be considerably overestimated for $v_{\rm w} \lesssim 0.1$ (dotted curve). We could also show that taking the Higgs bosons into account or not does not play a significant role. The same holds for the source terms proportional to the first-order perturbations $\mu_{t,1}$ and $u_{t,1}$, which we have neglected in the current paper. Their effect on the total baryon asymmetry is less than 10% in the model under consideration.

Let us finally discuss the dependence of η_B on the Higgs masses. Figure 7 shows contours of constant baryon asymmetry in the m_h–m_H plane, where we have fixed the parameters $\mu_3^2 = 10000\ {\rm GeV}^2$ and $\alpha = 0.2$. For each mass combination we determine all quantities relevant for the phase transition, such as ξ, $\tan\beta_T$, $L_{\rm w}$, $\theta_{\rm sym}$ and $\theta_{\rm brk}$ to put them into the transport equations. There is only a mild $v_{\rm w}$ dependence of the baryon asymmetry (cf. figure 6), so we consider only one wall velocity, $v_{\rm w} = 0.1$. In addition, the (ξ=1)-contour of figure 2 is also shown for orientation. As we increase m_H, leaving m_h fixed, the asymmetry becomes larger. This behavior results from the $m_t^2 \sim \xi^2$ dependence of the top source term. Accordingly the baryon asymmetry becomes larger for a stronger phase transition. If we increase m_h, leaving the heavy Higgs mass fixed, η_B becomes smaller and reaches a minimum at $m_h \approx 150$–160 GeV, similar to the behavior of $L_{\rm w}$. But in general there is only a minor dependence on the light Higgs mass. In this parameter setting it is possible to generate the observed baryon asymmetry for a heavy Higgs mass between 320 and 330 GeV and a light Higgs mass up to 160 GeV. Since η_B is more or less proportional to the CP-violating phase α, the measured value can also be explained for other values of the parameters if we adjust α. Then the heavy Higgs mass should be somewhat larger.

Comparing figures 5 and 7, we can use the baryon asymmetry to predict the EDMs. We see that for $\xi \sim 1$ and $m_h = 115$ GeV the neutron EDM is a factor of about 2 above the experimental bound, which including the theoretical uncertainties is marginally tolerable.

The electron EDM is a factor of about 5 below the experimental bound. Moving along the ($\xi = 1$)-contour to the largest Higgs mass of 190 GeV, we find $|d_e| \sim 0.03 \times 10^{-27} e$ cm and $|d_n| \sim 0.7 \times 10^{-26} e$ cm. Finally, taking $m_h = 190$ GeV and $m_H = 400$ GeV, we find $|d_e| \sim 3 \times 10^{-30} e$ cm and $|d_n| \sim 0.09 \times 10^{-26} e$ cm. So the experimental bound on the neutron EDM starts to cut into the parameter space of the model. Improving the bound by an order of magnitude would probe the larger part of the parameter space. The electron EDM is typically one to two orders of magnitude below the current bound.

In this paper we focused on the case $\tan\beta = 1$. As we discussed in the context of eq. (3.4), larger values of $\tan\beta$ will lead to a smaller value of the baryon asymmetry, since the change in θ is then mostly due to a change in θ_1 rather than θ_2. Extrapolating from the example of figure 7, we estimate that for $\tan\beta \gtrsim 10$, successful baryogenesis should in any case be in conflict with the EDM bounds. It would be interesting to check this issue by direct evaluations.

So there exists a wide range of realistic parameters where the computation of η_B is under control, and which yields the observed baryon asymmetry.

7. Conclusions

We have studied electroweak baryogenesis in the 2HDM, focusing on the case of $\tan\beta = 1$ and degenerate extra Higgs states. Evaluating the thermal Higgs potential in the one-loop approximation, we find a first-order phase transition, which is strong enough to avoid baryon number washout. This is achieved by the loop-contributions of the extra Higgs states, provided they are sufficiently strongly coupled. Taking $\mu_3^2 = 10000$ GeV^2, this happens for a heavy Higgs mass $m_H \gtrsim 300$ GeV. The mass of the light, SM-like Higgs, m_h, can be up to 200 GeV, or even larger. The Higgs potential allows the introduction of a single CP-violating phase, which has only a minor impact on the strength of the phase transition. In our example, if m_H reaches about 500 GeV, the phase transition becomes very strong, while the perturbative description starts to break down. These findings are in agreement with those of ref. [21].

We have computed the properties of the phase boundary. The walls are typically thick, but the width decreases with larger m_H from $L_\mathrm{w} \sim 15 T_c^{-1}$ to about $2T_c^{-1}$. We also compute the profile of the relative complex phase between the two Higgs vevs, which changes by an amount $\Delta\theta$ between the broken and the symmetric phase.

This phase shift leads to a CP-violating source term for the top quark, which drives the generation of the baryon asymmetry. We compute the source term in the WKB approximation and solve the resulting transport equations, using the formalism of ref. [14]. We find that for typical parameter values the baryon asymmetry is in the range of the observed value. The explicit CP phase in the Higgs potential has to be taken between 10^{-2} and unity. For larger values of m_H the baryon asymmetry increases, as the phase transition becomes stronger and the wall thinner. Our result differs from those of ref. [16]. There the baryon asymmetry in the 2HDM was computed using the method of reflection and transmission coefficients. In the regime of thick walls, this method is known not to give the leading contribution to the baryon asymmetry, which explains the different results.

JHEP11(2006)038

We have also computed the EDMs of the electron and neutron. Since there is only a single complex phase in the model, we can predict $|d_e|$ and $|d_n|$ in terms of the baryon asymmetry and the Higgs masses. We find that $|d_n| \gtrsim 10^{-27} e$ cm. For the smallest allowed values of m_h and m_H, $|d_n|$ can slightly exceed the experimental bound. Improving the neutron EDM sensitivity by an order of magnitude would test a substantial part of the parameter space of the model. The electron EDM is typically one to two orders of magnitude below the bound. These values are for $\tan\beta = 1$. Extrapolating our results suggests that for $\tan\beta \gtrsim 10$, the 2HDM cannot produce the observed baryon asymmetry without being in conflict with the EDM constraints. In any case, the 2HDM can explain the baryon asymmetry for a considerable range of the model parameters.

It would be interesting to extend our investigations to cover the full parameter space, in particular the case $\tan\beta > 1$. Since for larger values of m_H higher-order corrections to the effective potential become more and more important, these contributions should be studied in more detail, most reliably on the lattice. Our proposal is testable at the LHC in the sense that at least one Higgs state should be observed. Furthermore, CP violation may be detectable in top pair production [55, 31]. Stringent tests could be performed at a future e^+e^- linear collider, where for instance deviations in the Higgs self-coupling could be detected [56].

Acknowledgments

We thank D. Bödeker, J. Erdmann, M. Laine, A. Ritz and S. Weinstock for valuable discussions.

References

[1] D.N. Spergel et al., *Wilkinson microwave anisotropy probe (WMAP) three year results: implications for cosmology*, astro-ph/0603449.

[2] A.D. Sakharov, *Violation of CP invariance, c asymmetry and baryon asymmetry of the universe*, *Pisma Zh. Eksp. Teor. Fiz.* **5** (1967) 32–35, [*JETP Lett.* **5** (1967) 24].

[3] V.A. Kuzmin, V.A. Rubakov and M.E. Shaposhnikov, *On the anomalous electroweak baryon number nonconservation in the early universe*, *Phys. Lett.* **B 155** (1985) 36.

[4] K. Kajantie, M. Laine, K. Rummukainen and M.E. Shaposhnikov, *Is there a hot electroweak phase transition at $M_h \approx M_w$?*, *Phys. Rev. Lett.* **77** (1996) 2887 [hep-ph/9605288]; *A non-perturbative analysis of the finite t phase transition in* SU(2)× *U(1) electroweak theory*, *Nucl. Phys.* **B 493** (1997) 413 [hep-lat/9612006];
F. Csikor, Z. Fodor and J. Heitger, *Endpoint of the hot electroweak phase transition*, *Phys. Rev. Lett.* **82** (1999) 21 [hep-ph/9809291].

[5] LEP collaboration, *A combination of preliminary electroweak measurements and constraints on the standard model*, hep-ex/0312023.

[6] M.B. Gavela, P. Hernandez, J. Orloff, O. Pene and C. Quimbay, *Standard model CP-violation and baryon asymmetry, part 2. Finite temperature*, *Nucl. Phys.* **B 430** (1994) 382 [hep-ph/9406289];

P. Huet and E. Sather, *Electroweak baryogenesis and standard model CP-violation*, *Phys. Rev.* **D 51** (1995) 379 [hep-ph/9404302];
T. Konstandin, T. Prokopec and M.G. Schmidt, *Axial currents from CKM matrix CP-violation and electroweak baryogenesis*, *Nucl. Phys.* **B 679** (2004) 246 [hep-ph/0309291].

[7] For a review, see: M. Trodden, *Electroweak baryogenesis*, *Rev. Mod. Phys.* **71** (1999) 1463 [hep-ph/9803479].

[8] M. Carena, M. Quiros and C.E.M. Wagner, *Opening the window for electroweak baryogenesis*, *Phys. Lett.* **B 380** (1996) 81 [hep-ph/9603420];
D. Delepine, J.M. Gerard, R. Gonzalez Felipe and J. Weyers, *A light stop and electroweak baryogenesis*, *Phys. Lett.* **B 386** (1996) 183 [hep-ph/9604440];
D. Bödeker, P. John, M. Laine and M.G. Schmidt, *The 2-loop MSSM finite temperature effective potential with stop condensation*, *Nucl. Phys.* **B 497** (1997) 387 [hep-ph/9612364];
B. de Carlos and J.R. Espinosa, *The baryogenesis window in the MSSM*, *Nucl. Phys.* **B 503** (1997) 24 [hep-ph/9703212];
M. Laine and K. Rummukainen, *The MSSM electroweak phase transition on the lattice*, *Nucl. Phys.* **B 535** (1998) 423 [hep-lat/9804019].

[9] J.M. Cline and K. Kainulainen, *A new source for electroweak baryogenesis in the MSSM*, *Phys. Rev. Lett.* **85** (2000) 5519 [hep-ph/0002272];
J.M. Cline, M. Joyce and K. Kainulainen, *Supersymmetric electroweak baryogenesis*, *JHEP* **07** (2000) 018 [hep-ph/0006119], Erratum added online, Oct/2/2001.

[10] M. Carena, J.M. Moreno, M. Quiros, M. Seco and C.E.M. Wagner, *Supersymmetric CP-violating currents and electroweak baryogenesis*, *Nucl. Phys.* **B 599** (2001) 158 [hep-ph/0011055];
S.J. Huber, P. John and M.G. Schmidt, *Bubble walls, CP-violation and electroweak baryogenesis in the MSSM*, *Eur. Phys. J.* **C 20** (2001) 695 [hep-ph/0101249];
M. Carena, M. Quiros, M. Seco and C.E.M. Wagner, *Improved results in supersymmetric electroweak baryogenesis*, *Nucl. Phys.* **B 650** (2003) 24 [hep-ph/0208043];
T. Konstandin, T. Prokopec and M.G. Schmidt, *Kinetic description of fermion flavor mixing and CP- violating sources for baryogenesis*, *Nucl. Phys.* **B 716** (2005) 373 [hep-ph/0410135];
T. Konstandin, T. Prokopec, M.G. Schmidt and M. Seco, *MSSM electroweak baryogenesis and flavour mixing in transport equations*, *Nucl. Phys.* **B 738** (2006) 1 [hep-ph/0505103];
V. Cirigliano, M.J. Ramsey-Musolf, S. Tulin and C. Lee, *Yukawa and tri-scalar processes in electroweak baryogenesis*, *Phys. Rev.* **D 73** (2006) 115009 [hep-ph/0603058].

[11] M. Pietroni, *The electroweak phase transition in a nonminimal supersymmetric model*, *Nucl. Phys.* **B 402** (1993) 27 [hep-ph/9207227];
A.T. Davies, C.D. Froggatt and R.G. Moorhouse, *Electroweak baryogenesis in the next to minimal supersymmetric model*, *Phys. Lett.* **B 372** (1996) 88 [hep-ph/9603388];
S.J. Huber and M.G. Schmidt, *SUSY variants of the electroweak phase transition*, *Eur. Phys. J.* **C 10** (1999) 473 [hep-ph/9809506]; *Electroweak baryogenesis: concrete in a SUSY model with a gauge singlet*, *Nucl. Phys.* **B 606** (2001) 183 [hep-ph/0003122];
M. Bastero-Gil, C. Hugonie, S.F. King, D.P. Roy and S. Vempati, *Does lep prefer the nmssm?*, *Phys. Lett.* **B 489** (2000) 359 [hep-ph/0006198];
A. Menon, D.E. Morrissey and C.E.M. Wagner, *Electroweak baryogenesis and dark matter in the nmssm*, *Phys. Rev.* **D 70** (2004) 035005 [hep-ph/0404184];
S.W. Ham, Y.S. Jeong and S.K. Oh, *Electroweak phase transition in an extension of the standard model with a real Higgs singlet*, *J. Phys.* **G 31** (2005) 857 [hep-ph/0411352].

JHEP11(2006)038

[12] X.-M. Zhang, *Operators analysis for Higgs potential and cosmological bound on Higgs mass*, *Phys. Rev.* **D 47** (1993) 3065 [hep-ph/9301277];
C. Grojean, G. Servant and J.D. Wells, *First-order electroweak phase transition in the standard model with a low cutoff*, *Phys. Rev.* **D 71** (2005) 036001 [hep-ph/0407019];
S.W. Ham and S.K. Oh, *Electroweak phase transition in the standard model with a dimension-six Higgs operator at one-loop level*, *Phys. Rev.* **D 70** (2004) 093007 [hep-ph/0408324].

[13] D. Bödeker, L. Fromme, S.J. Huber and M. Seniuch, *The baryon asymmetry in the standard model with a low cut-off*, *JHEP* **02** (2005) 026 [hep-ph/0412366].

[14] L. Fromme and S.J. Huber, *Top transport in electroweak baryogenesis*, hep-ph/0604159.

[15] A.G. Cohen, D.B. Kaplan and A.E. Nelson, *Spontaneous baryogenesis at the weak phase transition*, *Phys. Lett.* **B 263** (1991) 86;
A.E. Nelson, D.B. Kaplan and A.G. Cohen, *Why there is something rather than nothing: matter from weak interactions*, *Nucl. Phys.* **B 373** (1992) 453.

[16] J.M. Cline, K. Kainulainen and A.P. Vischer, *Dynamics of two Higgs doublet CP-violation and baryogenesis at the electroweak phase transition*, *Phys. Rev.* **D 54** (1996) 2451 [hep-ph/9506284].

[17] A.I. Bochkarev, S.V. Kuzmin and M.E. Shaposhnikov, *Electroweak baryogenesis and the Higgs boson mass problem*, *Phys. Lett.* **B 244** (1990) 275; *On the model dependence of the cosmological upper bound on the Higgs boson and top quark masses*, *Phys. Rev.* **D 43** (1991) 369.

[18] N. Turok and J. Zadrozny, *Electroweak baryogenesis in the two doublet model*, *Nucl. Phys.* **B 358** (1991) 471; *Phase transitions in the two doublet model*, *Nucl. Phys.* **B 369** (1992) 729.

[19] K. Funakubo, A. Kakuto and K. Takenaga, *The effective potential of electroweak theory with two massless Higgs doublets at finite temperature*, *Prog. Theor. Phys.* **91** (1994) 341 [hep-ph/9310267].

[20] A.T. Davies, C.D. froggatt, G. Jenkins and R.G. Moorhouse, *Baryogenesis constraints on two Higgs doublet models*, *Phys. Lett.* **B 336** (1994) 464.

[21] J.M. Cline and P.-A. Lemieux, *Electroweak phase transition in two Higgs doublet models*, *Phys. Rev.* **D 55** (1997) 3873 [hep-ph/9609240].

[22] M. Joyce, T. Prokopec and N. Turok, *Electroweak baryogenesis from a classical force*, *Phys. Rev. Lett.* **75** (1995) 1695 [hep-ph/9408339]; *Nonlocal electroweak baryogenesis, part 2. The classical regime*, *Phys. Rev.* **D 53** (1996) 2958 [hep-ph/9410282].

[23] T. Prokopec, M.G. Schmidt and S. Weinstock, *Transport equations for chiral fermions to order h-bar and electroweak baryogenesis*, *Ann. Phys. (NY)* **314** (2004) 208 [hep-ph/0312110]; *Transport equations for chiral fermions to order h-bar and electroweak baryogenesis, II*, *Ann. Phys. (NY)* **314** (2004) 267 [hep-ph/0406140].

[24] S.L. Glashow and S. Weinberg, *Natural conservation laws for neutral currents*, *Phys. Rev.* **D 15** (1977) 1958.

[25] M. Sher, *Electroweak Higgs potentials and vacuum stability*, *Phys. Rept.* **179** (1989) 273;
J.F. Gunion, H.E. Haber, G.L. Kane and S. Dawson, *The Higgs Hunter's Guide*, Addison-Wesley, Reading-MA, 1990.

JHEP11(2006)038

[26] G.C. Branco and M.N. Rebelo, *The Higgs mass in a model with two scalar doublets and spontaneous CP-violation*, *Phys. Lett.* **B 160** (1985) 117.

[27] P.M. Ferreira, R. Santos and A. Barroso, *Stability of the tree-level vacuum in two Higgs doublet models against charge or CP spontaneous violation*, *Phys. Lett.* **B 603** (2004) 219 [hep-ph/0406231].

[28] M. Maniatis, A. von Manteuffel, O. Nachtmann and F. Nagel, *Stability and symmetry breaking in the general two-higgs- doublet model*, hep-ph/0605184.

[29] C.D. Froggatt, R.G. Moorhouse and I.G. Knowles, *Leading radiative corrections in two scalar doublet models*, *Phys. Rev.* **D 45** (1992) 2471.

[30] M. Neubert, *Renormalization-group improved calculation of the $B \to X/s + \gamma$ branching ratio*, *Eur. Phys. J.* **C 40** (2005) 165 [hep-ph/0408179].

[31] A.W. El Kaffas, W. Khater, O. Magne Ogreid and P. Osland, *Consistency of the two Higgs doublet model and CP-violation in top production at the LHC*, hep-ph/0605142.

[32] K. Cheung and O.C.W. Kong, *Can the two-Higgs-doublet model survive the constraint from the muon anomalous magnetic moment as suggested?*, *Phys. Rev.* **D 68** (2003) 053003 [hep-ph/0302111].

[33] M. Krawczyk and D. Temes, *$2HDM(II)$ radiative corrections in leptonic tau decays*, *Eur. Phys. J.* **C 44** (2005) 435 [hep-ph/0410248].

[34] L. Dolan and R. Jackiw, *Symmetry behavior at finite temperature*, *Phys. Rev.* **D 9** (1974) 3320.

[35] K. Kajantie, M. Laine, K. Rummukainen and M.E. Shaposhnikov, *The electroweak phase transition: a non-perturbative analysis*, *Nucl. Phys.* **B 466** (1996) 189 [hep-lat/9510020]; M. Laine and K. Rummukainen, *Two Higgs doublet dynamics at the electroweak phase transition: a non-perturbative study*, *Nucl. Phys.* **B 597** (2001) 23 [hep-lat/0009025].

[36] G.D. Moore, *Measuring the broken phase sphaleron rate nonperturbatively*, *Phys. Rev.* **D 59** (1999) 014503 [hep-ph/9805264].

[37] T. Konstandin and S.J. Huber, *Numerical approach to multi dimensional phase transitions*, *JCAP* **06** (2006) 021 [hep-ph/0603081].

[38] S.J. Huber, P. John, M. Laine and M.G. Schmidt, *CP-violating bubble wall profiles*, *Phys. Lett.* **B 475** (2000) 104 [hep-ph/9912278].

[39] C.A. Baker et al., *An improved experimental limit on the electric dipole moment of the neutron*, *Phys. Rev. Lett.* **97** (2006) 131801 [hep-ex/0602020].

[40] B.C. Regan, E.D. Commins, C.J. Schmidt and D. DeMille, *New limit on the electron electric dipole moment*, *Phys. Rev. Lett.* **88** (2002) 071805.

[41] S. Weinberg, *Larger Higgs exchange terms in the neutron electric dipole moment*, *Phys. Rev. Lett.* **63** (1989) 2333; *Unitarity constraints on CP nonconservation in Higgs exchange*, *Phys. Rev.* **D 42** (1990) 860.

[42] S.M. Barr and A. Zee, *Electric dipole moment of the electron and of the neutron*, *Phys. Rev. Lett.* **65** (1990) 21.

[43] W. Bernreuther and M. Suzuki, *The electric dipole moment of the electron*, *Rev. Mod. Phys.* **63** (1991) 313.

JHEP11(2006)038

[44] J.F. Gunion and R. Vega, *The electron electric dipole moment for a CP-violating neutral Higgs sector*, *Phys. Lett.* **B 251** (1990) 157.

[45] D. Chang, W.Y. Keung and T.C. Yuan, *Two loop bosonic contribution to the electron electric dipole moment*, *Phys. Rev.* **D 43** (1991) 14.

[46] R.G. Leigh, S. Paban and R.M. Xu, *Nucl. Phys.* **B352** 1991) 45.

[47] M. Pospelov and A. Ritz, *Electric dipole moments as probes of new physics*, *Ann. Phys. (NY)* **318** (2005) 119 [hep-ph/0504231].

[48] J.F. Gunion and D. Wyler, *Inducing a large neutron electric dipole moment via a quark chromoelectric dipole moment*, *Phys. Lett.* **B 248** (1990) 170.

[49] T. Hayashi, Y. Koide, M. Matsuda and M. Tanimoto, *Neutron electric dipole moment in two Higgs doublet model*, *Prog. Theor. Phys.* **91** (1994) 915 [hep-ph/9401331].

[50] D.A. Dicus, *Neutron electric dipole moment from charged Higgs exchange*, *Phys. Rev.* **D 41** (1990) 999.

[51] M. Chemtob, *Nucleon electric dipole moment and gluonic content of light hadrons*, *Phys. Rev.* **D 45** (1992) 1649.

[52] G.D. Moore, *Sphaleron rate in the symmetric electroweak phase*, *Phys. Rev.* **D 62** (2000) 085011 [hep-ph/0001216].

[53] G.D. Moore, *Computing the strong sphaleron rate*, *Phys. Lett.* **B 412** (1997) 359 [hep-ph/9705248].

[54] P. Huet and A.E. Nelson, *Electroweak baryogenesis in supersymmetric models*, *Phys. Rev.* **D 53** (1996) 4578 [hep-ph/9506477].

[55] W. Bernreuther and A. Brandenburg, *Tracing CP-violation in the production of top quark pairs by multiple TeV proton proton collisions*, *Phys. Rev.* **D 49** (1994) 4481 [hep-ph/9312210].

[56] A. Djouadi, W. Kilian, M. Muhlleitner and P.M. Zerwas, *Testing Higgs self-couplings at e^+e^- linear colliders*, *Eur. Phys. J.* **C 10** (1999) 27 [hep-ph/9903229];
S. Kanemura, Y. Okada and E. Senaha, *Electroweak baryogenesis and quantum corrections to the triple Higgs boson coupling*, *Phys. Lett.* **B 606** (2005) 361 [hep-ph/0411354];
S.W. Ham and S.K. Oh, *Electroweak phase transition and Higgs self-couplings in the two-Higgs-doublet model*, hep-ph/0502116.

JHEP11(2006)038

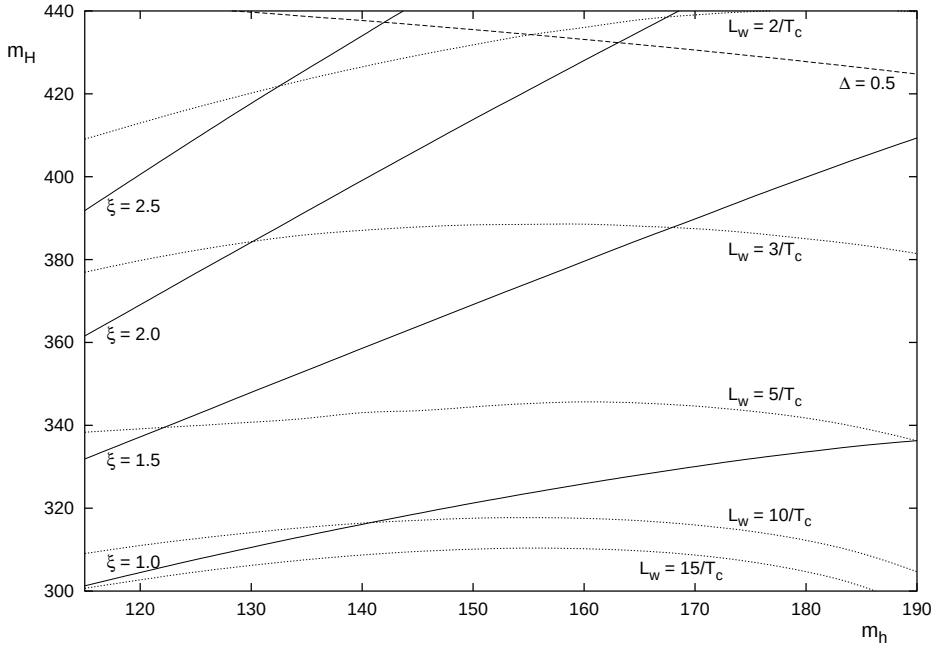

Figure 1: Lines of constant ξ and $L_{\rm w}$ in the m_h-m_H-plane for $\mu_3^2 = 10000$ GeV^2 and $\alpha = 0$. In addition, the line of the relative size of the one-loop corrections $\Delta = \max|\delta\lambda_i/\lambda_i| = 0.5$ is shown. The Higgs masses are given in units of GeV.

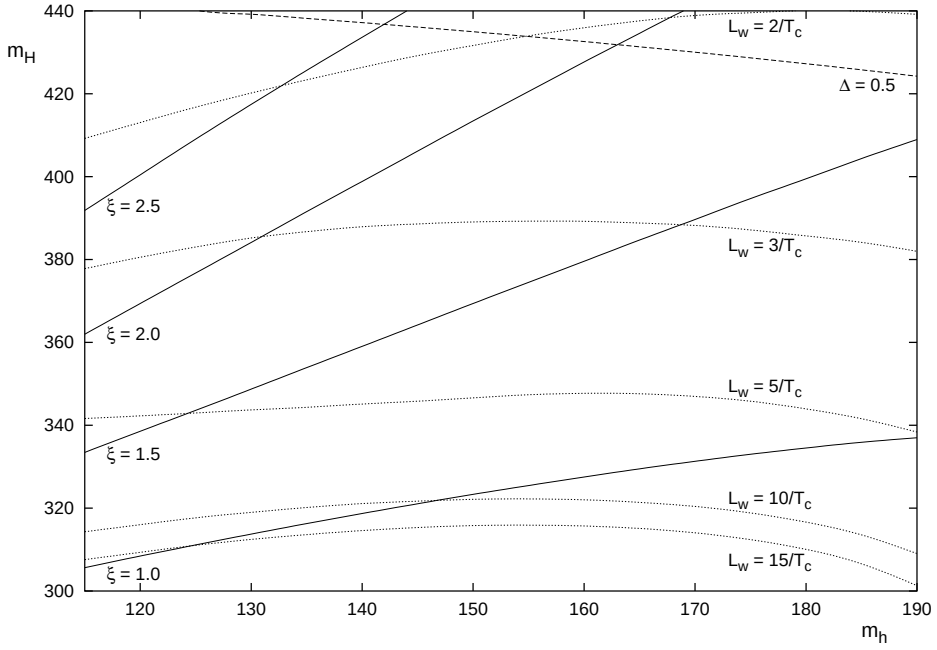

Figure 2: The same plot as in figure 1, but for the set $\mu_3^2 = 10000$ GeV^2 and $\alpha = 0.2$.

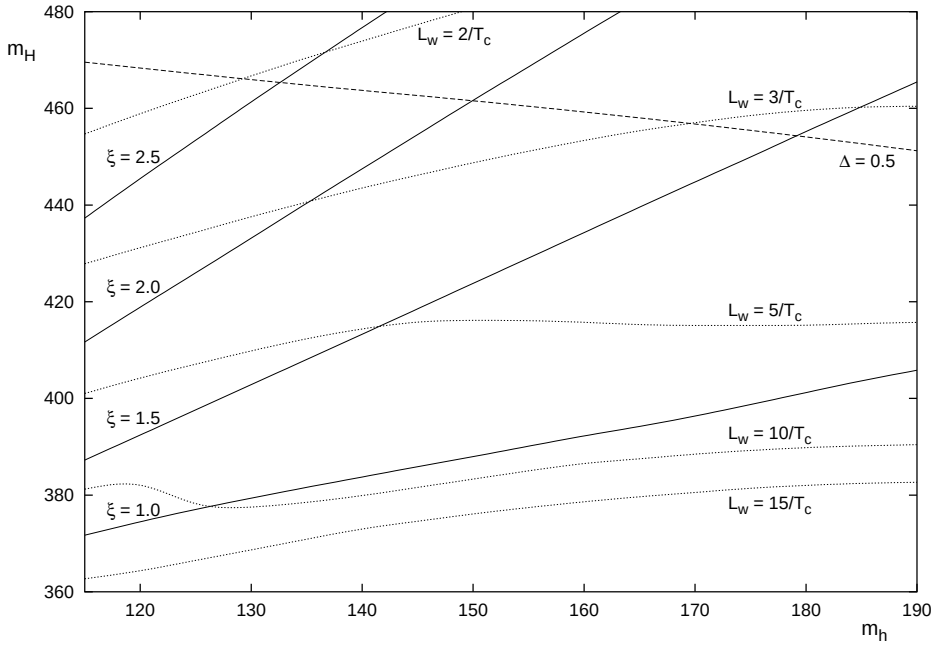

Figure 3: The same plot as in figures 1 and 2, but for $\mu_3^2 = 20000$ GeV^2 and $\alpha = 0.2$

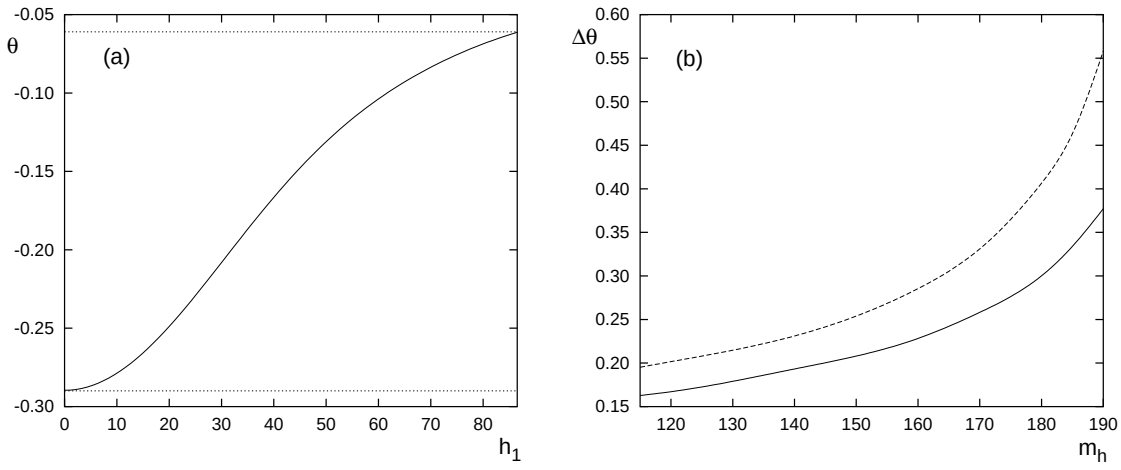

Figure 4: The phase θ and the difference $\Delta\theta$ for the set $\mu_3^2 = 10000$ GeV^2, $\alpha = 0.2$.
(a) The change of θ during the PT, as a function of h_1 (given in GeV), at fixed $m_h = 150$ GeV, $m_H = 350$ GeV.
(b) $\Delta\theta$ versus m_h (given in GeV) for $m_H = 330$ GeV (solid) and 400 GeV (dashed).

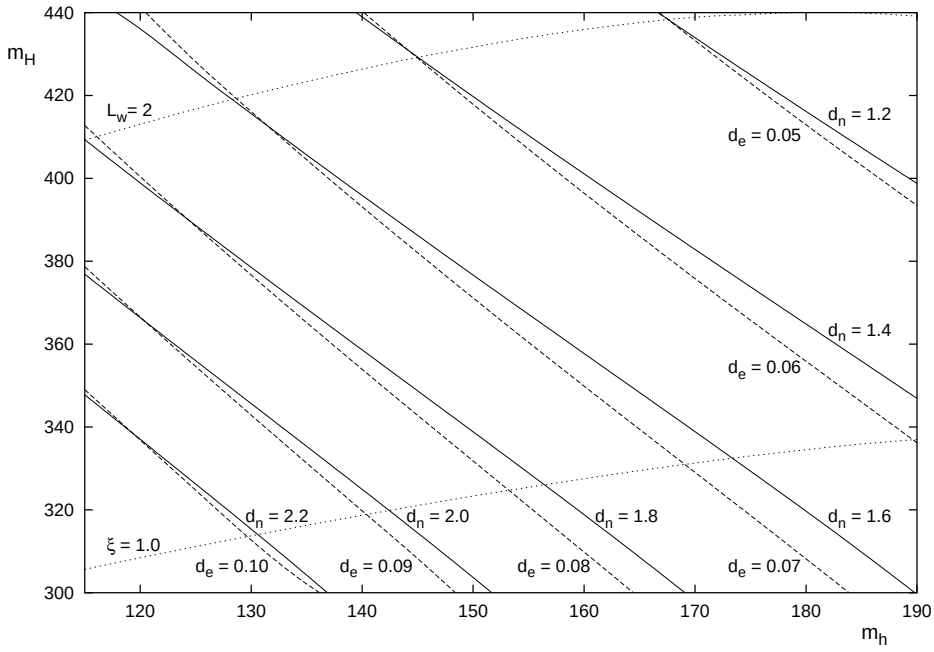

Figure 5: Lines of constant neutron (solid) and electron EDMs (dashed) for the set $\mu_3^2 = 10000\ \mathrm{GeV}^2$, $\alpha = 0.2$, d_n is given in units of $10^{-26}\ e\,\mathrm{cm}$, d_e in units of $10^{-27}\ e\,\mathrm{cm}$, and Higgs masses in GeV. The lower dotted line indicates the bound $\xi = 1$, the upper one $L_\mathrm{w} = 2$.

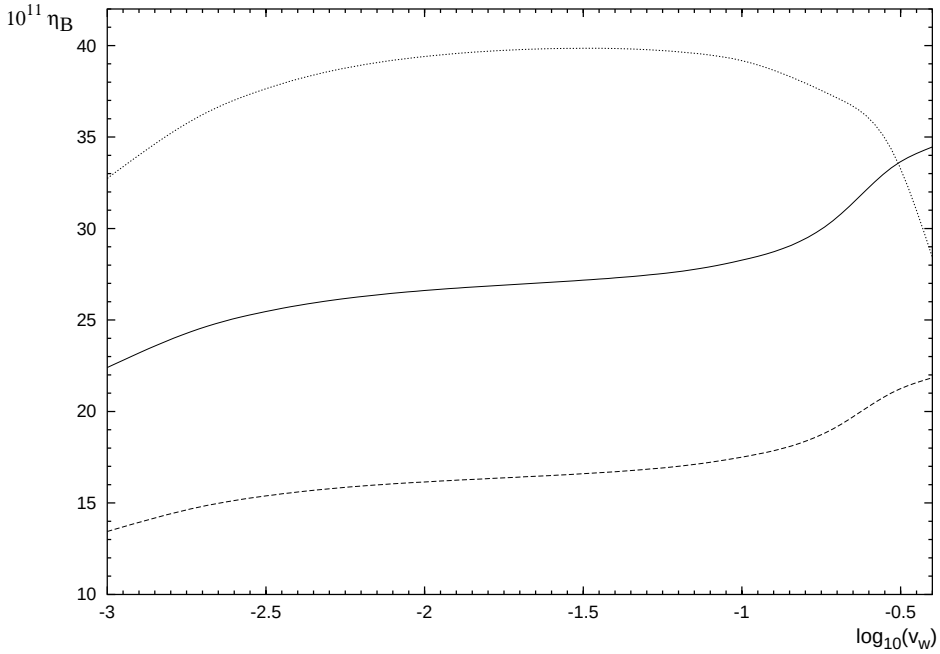

Figure 6: The solid line represents η_B as a function of the wall velocity for $m_h = 125$ GeV, $m_H = 350$ GeV, $\mu_3^2 = 10000\ \mathrm{GeV}^2$ and $\alpha = 0.2$. This parameter setting determines $L_\mathrm{w} = 4.5/T$ and $\xi = 1.6$. The dashed line would be the asymmetry when we substitute $E_{0z} \to E_0$ in the dispersion relations. The dotted curve corresponds to the case where the W-scatterings are in equilibrium.

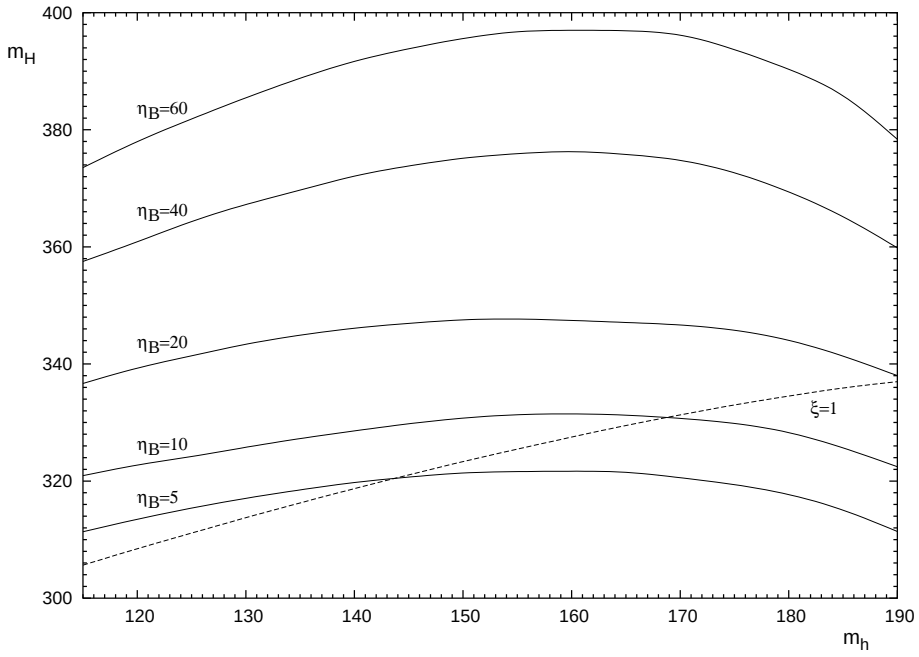

Figure 7: Contours of constant η_B in the m_h–m_H plane for $\mu_3^2 = 10000$ GeV^2 and $\alpha = 0.2$. The Higgs masses are given in units of GeV and η_B in units of 10^{-11}.